Contribution from the Kenan Laboratories of Chemistry,
The University of North Carolina, Chapel Hill, North Carolina 27514

Carbon-13, Oxygen-17, and Molybdenum-95 Nuclear Magnetic Resonance Studies of Oxomolybdenum(VI) Complexes

MICHAEL A. FREEMAN, FRANKLIN A. SCHULTZ,[1] and CHARLES N. REILLEY*

Ligands which contain three facially arranged amine, carboxylate, and/or heterocyclic nitrogen functional groups form stable complexes with the MoO_3 core at pH ~6. ^{13}C and ^{17}O NMR spectra reveal an interesting variety of compositions, inter- and intramolecular labilities, and spatial arrangements of ligand framework and donor atoms for these complexes. Ligands which contain a hydroxyl functional group result in the formation of $Mo_2O_5{}^{2+}$ dimers. The hydroxyl proton is lost upon coordination, and the strong trans influence of the coordinated alkoxy group weakens the opposing $Mo=O$ bond and causes formation of a μ-oxo-bridged $Mo_2O_5{}^{2+}$ core. A ranking of trans-influencing ability of common ligand groups is derived from crystal structure data and is shown to be a controlling factor in the structure and composition of oxomolybdenum(VI) complexes. Oxygen-17 NMR chemical shifts of MoO_3–ligand complexes are much more sensitive to trans influences than crystal structure distance measurements. The [17]O chemical shifts of oxomolybdenum(VI) complexes and polyanions reported in the literature reveal a smooth, nonlinear relation to Mo–O bond length. [95]Mo NMR chemical shifts of MoO_3–ligand complexes are identical within experimental error, and line widths show no relation to complex size.

Introduction

Molybdenum plays a key role in a number of important enzyme systems[2] and industrial catalysts.[3] A detailed knowledge of its coordination chemistry is essential to understanding the mechanistic role it plays in these catalytic processes. While the lower oxidation states Mo(II)–Mo(V) are pertinent to the above processes, the most stable aqueous oxidation state is Mo(VI).[4] The coordination chemistry of this oxidation state is important in that it must play a crucial role in the transport of molybdenum from its natural aqueous environment into its ultimate form in biological systems.

The literature reveals a growing understanding of the principal features of molybdenum(VI) chemistry. Regularities in structure and reactivity of Mo(VI) compounds are widely noted and are summarized in the following observations.

(1) Ligand to Metal Multiple Bonds Are Almost Universally Present. Terminal oxo groups are ubiquitous ligands in aqueous environments,[4] and multiply bonded S and N groups are also known.[2] When two or three such ligands occur, they occupy mutually cis positions.[5]

(2) Multiple Bonding to a Given Ligand Is at the Expense of Bonds to Other Ligands. Four multiply bonded groups result in exclusion of other ligands and formation of tetrahedral species such as $MoO_4{}^{2-}$. When fewer such groups are present, other ligands may coordinate and the individual bonds to each multiply bonded ligand become stronger. Thus the average Mo–O bond distance decreases in the order[6] $MoO_4 > MoO_3L_3 > MoO_2L_4 > MoOL_5$. The additional ligands, if not identical, will arrange themselves with the weaker π-bonding ligands trans to the multiply bonded groups and the stronger π-bonding ligands cis to the multiply bonded groups and trans to one another. Competition for metal $d\pi$ orbitals is minimized by this arrangement. Further, bonds to ligands trans to multiply bonded dentates are lengthened and weakened[7] (vide infra).

(3) Octahedral Coordination Predominates.[2,5] Nonoctahedral Mo(VI) compounds occur when (a) four strongly π-donating groups are present, (b) chelate size and steric constraints

disfavor occupation of octahedral sites, or (c) interligand steric hindrances or dentate–dentate bonding disfavor normal ligand arrangements. Chelates of very small ring size such as peroxo and dithiocarbamato ligands lead to pentagonal-bipyramidal forms.[6,8] Bulky substituents on the chelate ring can lead to a skew trapezoidal-bipyramidal form[9] whereas analogous, but less bulky ligands produce pseudooctahedra.[10] Bonding between coordinated atoms, as between the sulfur atoms of tris(dithiolene) complexes, can stabilize trigonal prismatic[11] rather than octahedral forms.

(4) Strong Trans Influences Are Observed at Sites Trans to Strongly Bonded Ligands.[2,7] Trans influence is the weakening and lengthening of a bond trans to a given ligand.[12] Crystallographic measurements of bond lengths have established a trans influence series[13] CO, $N_2 < NO < RN^{-2} < O^{2-} < N^{3-}$, which shows increasing effect with formation of retrodative $(L \leftarrow M) < \text{donor } (L \rightarrow M) < \text{covalent } (L–M)$ bonds. An extended Hückel treatment of the trans-influencing ability of ligands shows that the ligand with better orbital overlap with the metal ion and covalent bonding ability destabilizes the bond opposite to itself while enhancing the stability of its own bond.[14]

(5) Multiply Bonded Oxo Ligands Are Subject to Protonation and Elimination. Tetrahedral $MoO_4{}^{2-}$ exists at high pH in solution, but with lower pH protonation occurs and the complex is thought to become six-coordinate[15] en route to oligomeric paramolybdate by a condensation reaction[1,16]

$$7MoO_4{}^{2-} + 8H^+ \rightleftharpoons Mo_7O_{24}{}^{6-} + H_2O$$
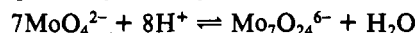
Similarly, the oxo ligands in complexes undergo protonation and condensation to produce μ-oxo species.[17]

The current paper is directed toward elucidating the relationship between ligand structure and complex-forming ability for oxomolybdenum–ligand species. We report here ^{13}C, [17]O, and [95]Mo nuclear magnetic resonance studies of Mo(VI) coordination to a number of chelating ligands containing amine,

(1) On sabbatical leave from Florida Atlantic University, Boca Raton, FL.
(2) Stiefel, E. I. *Progr. Inorg. Chem.* **1977**, *22*, 1.
(3) "Proceedings of the Third International Conference on the Chemistry and Uses of Molybdenum"; Barry, H. F., Mitchell, P. C. H., Eds.; Climax Molbdenum Co.: Ann Arbor, MI, 1979; pp 73–236.
(4) Baes, C. F.; Mesmer, R. E. "The Hydrolysis of Cations"; Wiley: New York, 1976.
(5) Butcher, R. J.; Penfold, B. R.; Sinn, E. *J. Chem. Soc., Dalton Trans.* **1979**, 668.
(6) Spivack, B.; Dori, Z. *Coord. Chem. Rev.* **1975**, *17*, 99.
(7) Blake, A. B.; Cotton, F. A. *J. Am. Chem. Soc.* **1964**, *86*, 3024.

(8) Hursthourse, M. B.; Motevalli, M. *J. Chem. Soc., Dalton Trans.* **1979**, 1362.
(9) Stiefel, E. I.; Miller, K. F.; Bruce, A. E.; Corbin, J. L.; Berg, J. M.; Hodgson, K. O. *J. Am. Chem. Soc.* **1980**, *102*, 3624.
(10) Berg, J. M.; Hodgson, K. O.; Cramer, S. P.; Corbin, J. L.; Elsberry, A.; Paranya, N.; Stiefel, E. I. *J. Am. Chem. Soc.* **1979**, *101*, 2774.
(11) Bennet, M. J.; Cowie, M.; Martin, J. L.; Takats, J. *J. Am. Chem. Soc.* **1973**, *95*, 7504.
(12) Appleton, T. G.; Clark, H. C.; Manzer, L. E. *Coord. Chem. Rev.* **1973**, *10*, 335.
(13) Shustorovich, E. M.; Porai-Koshits, M. A.; Buslaev, Yu. A. *Coord. Chem. Rev.* **1975**, *17*, 1.
(14) Burdett, J. K.; Albright, T. A. *Inorg. Chem.* **1979**, *18*, 2112.
(15) Cruywagen, J. J.; Rohwer, E. F. C. H. *Inorg. Chem.* **1975**, *14*, 3136.
(16) Cruywagen, J. J. *Inorg. Chem.* **1980**, *19*, 552.
(17) Kula, R. J. *Anal. Chem.* **1966**, *38*, 1382.

Table I. Interaction of Ligands with Molybdenum(VI) at pH 6

no complexation	1:1 complexes	1:1 and 2:1 complexes
propylamine	aspartate (Asp)	ethylenediaminetetraacetic acid (EDTA)
acetic acid	N-methyl-N-(hydroxyethyl)glycine (MHEG)	1,2-propanediaminetetraacetic acid (PDTA)
diglycolic acid[a]	histidine (His)	(hydroxyethyl)ethylenediaminetriacetic acid (HEDTA)
glycine	iminodiacetic acid (IDA)	bis(β-aminoethyl) ether tetraacetic acid (EEDTA)
α-alanine	N-methyl-IDA (MIDA)	[ethylenebis(oxyethylenenitrilo)]tetraacetic acid (EGTA)
β-alanine	N-ethyl-IDA (EtIDA)	2-hydroxy-1,3-propanediaminetetraacetic acid (HPDTA)
dipicolinic acid (DPA)	N-benzyl-IDA (BzIDA)	diethylenetriaminepentaacetic acid (DTPA)
cyclohexanediaminetetraacetic acid (CYDTA)	N-(hydroxyethyl)-IDA (HEIDA)	
	nitrilotriacetic acid (NTA)	
	N,N'-ethylenediaminediacetic acid (N,N'-EDDA)	

[a] HOOCCH$_2$OCH$_2$COOH.

carboxylate, hydroxyl, and heterocyclic nitrogen functional groups, which explore the requirements for formation of stable oxomolybdenum(VI) complexes in terms of donor atom numbers, types, and spatial arrangements. This series of compounds also reveals several interesting stereochemical relationships between ligand framework and coordination geometry at the oxomolybdenum site. The trans influence of these and other ligand groups in oxomolybdenum(VI) chemistry is qualitatively estimated through intercomparison of bond lengths observed in crystal structures. A comparison of Mo–O bond lengths and ^{17}O NMR shifts for a number of oxomolybdenum(VI) complexes and polyanions reveals that the magnetic resonance experiment is the more sensitive to trans influences.

Experimental Section

The ligands utilized (Table I) were commercially available except for MHEG. PDTA was obtained from LaMont Laboratories and recrystallized from hot water before use. EEDTA, HEDTA, DTPA, and CYDTA were obtained from Geigy Chemicals and used as received, except for HEDTA, which was extracted with hot ethanol before use. The remaining ligands were obtained from Aldrich Chemical Co. and were used as received.

MHEG was synthesized from monochloroacetic acid and N-methylethanolamine by the method of Dwyer and Garvan.[18] Separation from the reaction mixture was accomplished by filtration of the reaction mixture, followed by adjustment to pH 7, filtration, and rotary evaporation of the filtrate to about $^1/_4$ volume. The resulting liquid was frozen in a high-vacuum distillation apparatus. After removal of water, the ligand was distilled as a lactone by the method of Vieles and Galsomias.[19] Care was taken to keep the heat source below 150 °C to avoid collection of a second, apparently oligomeric, product. The MHEG obtained after three distillations was pure, as evidenced from its ^{13}C NMR spectrum.

Solution samples for NMR spectroscopy were prepared by dissolving weighed amounts of ligand and Na$_2$MoO$_4$·2H$_2$O or (NH$_4$)$_6$Mo$_7$-O$_{24}$·4H$_2$O in 20% D$_2$O/80% H$_2$O to provide solutions 0.5 M in ligand. EtIDA solutions were saturated at somewhat lower molarity. The pH was adjusted to a value of 6 with 50% sodium hydroxide or 20% tetramethylammonium hydroxide solutions and concentrated sulfuric acid. Measured pH values were uncorrected for the D$_2$O content of the solvent.

NMR spectra were obtained with a Varian XL-100 spectrometer modified[20] for multinuclear observation at a magnetic field of 2.352 T (^{13}C, [95]Mo, and [17]O frequencies 25.16, 6.52, and 13.56 MHz). Carbon spectra were obtained from samples in 10-mm diameter tubes. A sweep width of 5120 Hz and an acquisition time of 0.800 s (8191 data points) were normally used, although a 1.600-s (16 384 data points) acquisition time was occasionally used to resolve some closely spaced lines. A Fourier transform data length of twice the acquired data length was used to produce as many displayed points as acquired.[21] Pulse length was 16 μs (~30° tip angle). Carbon chemical shifts were measured relative to internal dioxane and reported vs. Me$_4$Si with use of the relation[22] $\delta_{Me_4Si} = \delta_{dioxane} + 67.73$. Assignments of

carbon signals were accomplished by comparison to structurally similar molecules, by deuterium exchange at glycinate carbons using the method of Terrill and Reilley,[23] and proton-coupled spectra produced by gated decoupling. Molybdenum-95 spectra were obtained from samples in 18-mm tubes. Sweep widths of 100–2048 Hz were used with acquisition times of 1–0.031 s. Exponential weighting of FID's was routine. The line widths reported in Table V were measured in spectra where (acquisition time × Π)$^{-1}$ was much less than the measured line width. A pulse width of 105 μs provided the 90° tip angle used throughout. Fourier transform data lengths of at least twice acquired data length were routinely used. Molybdenum-95 chemical shifts were measured relative to a separate sample of 1 M Na$_2$MoO$_4$ in H$_2$O at pH 12. Viscosities were measured at 28 °C, the temperature at which [95]Mo spectra were obtained, with a Rheometrics torsional flow rheometer. Oxygen-17 NMR spectra were obtained with the same equipment as [95]Mo NMR spectra. The sweep width was 10 240 Hz, acquisition time was 0.5 s, 90° tip angle was from 100-μs rf pulse, and more than 10^5 transients were obtained for each spectrum. Chemical shifts were measured from the solvent water line, which was folded over into the spectrum.

Samples for pH titration were prepared in H$_2$O with stoichiometries and concentrations identical with those in the NMR samples. The proper stoichiometric amounts of each base were added to react with ligand protons, and the solutions were then titrated with 4.1 M nitric acid.

Results

[13]C Spectra of Oxomolybdenum(VI) Complexes. Table I gives a qualitative description of the interaction of each ligand with sodium molybdate at pH 6 as determined by ^{13}C NMR. Ligands are classified according to whether or not they form complexes with Mo(VI) and with respect to the metal:ligand stoichiometry of the resulting compounds. The ligands in the first column exhibit no new lines and no broadening or shift or existing lines and hence are classified as not forming complexes under these conditions. For the ligands in the second column, formation of 1:1 complexes is detected by the appearance of a set of new resonances which are distinct from the free ligand resonances over a range of Mo(VI):ligand ratios. These lines are generally sharp and therefore consistent with slow exchange of ligand between bound and unbound states on the NMR time scale. Only the Mo(VI)–His complex exhibits broad lines in its room-temperature ^{13}C spectrum and is considered to be intermolecularly labile. The Mo(VI)–NTA complex exhibits single lines for its glycinate and carboxylate carbon atoms. In agreement with an earlier study,[24] we attribute this observation to rapid intramolecular exchange of the glycinate arms in the complex. Most of the ligands in the second column of Table I form quite strong complexes with Mo(VI) as judged by virtually complete conversion of unbound to bound ligand resonances in solutions of 1:1 composition. A few ligands (Asp, His, MHEG) bind to Mo(VI) more weakly and have conversion efficiencies of 20–50% under the

(18) Dwyer, F. P.; Garvan, F. L. *J. Am. Chem. Soc.* **1959**, *81*, 2955.
(19) Vieles, P.; Galsomias, J. *Bull. Soc. Chim. Fr.* **1970**, *7*, 2529.
(20) Good, B. W. Ph.D. Thesis, The Unversity of North Carolina, 1978.
(21) Bartoldi, E.; Ernst, R. R. *J. Magn. Reson.* **1973**, *11*, 9.
(22) Sarneski, J. E.; Suprenant, H. L.; Molen, F. K.; Reilley, C. N. *Anal. Chem.* **1975**, *47*, 2116.
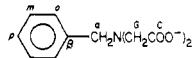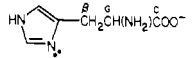(23) Terrill, J. B.; Reilley, C. N. *Anal. Chem.* **1966**, *38*, 1876.
(24) Miller, K. F.; Wentworth, R. A. D. *Inorg. Chem.* **1978**, *17*, 2769.

Table II

^{13}C NMR Chemical Shifts of Protonated and Complexed Forms of Ligands Which Form 1:1 Oxomolybdenum(VI) Complexes

ligand species	C	G	α	β	other
IDA	172.58	50.21			
MoIDA	180.88	57.56			
NTA	171.66	58.34			
MoNTA	178.92	65.49			
MIDA	170.90	59.74	43.58		
MoMIDA	179.12	66.99	51.64		
EtIDA	171.87	57.67	52.63	10.19	
MoEtIDA	179.30	63.39	58.84	10.09	
HEIDA	171.53	58.50	56.81	58.12	
MoHEIDA	179.29	64.24	64.78	59.04	
MHEG	171.33	59.78	42.82		58.98 56.69
MoMHEG-I	179.50	65.31	48.04		α′ 64.74 β′ 70.18
MoMHEG-II	179.32	64.04	48.30		65.18 70.02
BzIDA	171.41	57.37	60.04	131.33	o 130.43 m 132.18 p 130.23
MoBzIDA	178.77	63.71	67.11	134.15	132.24 129.82 130.01
His^a	174.13	55.26	27.43		Im 2 136.74 Im 4 132.80 Im 5 117.70
MoHis^a	182.76	55.26	29.04		137.80 133.30 116.00
Asp	178.67	53.27		37.77	C′ 175.46
MoAsp	182.84	53.40		39.10	178.40
N,N′-EDDA	172.43	50.97	44.75		
MoN,N′-EDDA-I	181.95	57.69	52.23		α₂ 48.38 G° 55.26 C° 178.50
MoN,N′-EDDA-II	181.47	55.90^b	51.38		47.98 55.90^b 178.24

Molecular Positions

IDA
$\overset{G\ \ \ C}{HN(CH_2COO^-)_2}$

NTA
$\overset{G\ \ \ C}{N(CH_2COO^-)_3}$

MIDA
$\overset{\alpha\ \ \ \ \ G\ \ \ C}{CH_3N(CH_2COO^-)_2}$

EtIDA
$\overset{\beta\ \ \ \ \alpha\ \ \ \ \ G\ \ \ C}{CH_3CH_2N(CH_2COO^-)_2}$

HEIDA
$HOCH_2CH_2N(CH_2COO^-)_2$

MHEG
$\overset{\alpha\ \ \ \ G\ \ \ C\ \ \ \ \ \alpha'\ \ \beta'}{CH_3N(CH_2CO_2^-)CH_2CH_2OH}$

BzIDA
(benzene ring labeled p, m, o, β, α) $-\overset{\alpha}{CH_2}N(\overset{G}{CH_2}\overset{C}{COO^-})_2$

HIS
(imidazole ring) $-\overset{\beta}{CH_2}\overset{\alpha}{CH(NH_2)}\overset{C}{COO^-}$

ASP
$\overset{C'\beta\ \ \ \ \ \ G\ \ \ \ \ \ \ \ \ C}{{}^-OOCCH_2CH(NH_2)COO^-}$

N,N′-EDDA
$\overset{C\ G\ \ \ \ \ \ \alpha_1\ \ \ \alpha_2\ \ \ \ \ \ G°\ \ C°}{{}^-OOCCH_2NHCH_2CH_2NHCH_2COO^-}$
Mo   Mo   Mo

^{a} At 5 °C. ^{b} Equilibrated by fast exchange.

same conditions. ^{13}C chemical shifts for all of these ligands in their monoprotonated and oxomolybdenum complex forms are shown in Table II.

The ligands in the third column of Table I contain more than one potential coordinating group and may form complexes with either 1:1 or 2:1 metal:ligand stoichiometry. The various species characteristics of this behavior are identified from ^{13}C spectra recorded as a function of Mo(VI):ligand ratio. The ^{13}C chemical shifts of the diprotonated and 1:1 and 2:1 complexed forms of these ligands are shown in Table III. In the case of the 1:1 complexes, the bound and unbound ligand groups exhibit different resonances. For example, the 1:1 Mo(VI)–EDTA complex exists as ($^-$O₂CCH₂)₂NH$^+$-CH₂|CH₂N(CH₂CO₂$^-$)₂$^{2-}$(MoO₃) and the ^{13}C resonances for the carbons on the left of the vertical bar are listed in Table III under a heading labeled "H$^+$", whereas the ^{13}C resonances for the carbons on the right of the vertical bar are listed under a heading labeled "MoO₃".

The 1:1 Mo(VI)–PDTA complex can exist in two forms because the iminodiacetate groups are nonequivalent and the Mo(VI) can bind to one or to the other group. The two forms are differentiated in Table III by use of the roman numerals I and II. Also, two forms of the Mo(VI)–ligand species have been identified in the case of the 2:1 Mo(VI)–HEDTA and 1:1 Mo(VI)–MHEG and Mo(VI)–N,N′-EDDA complexes, and these forms also are differentiated by the use of Roman numerals I and II.

^{95}Mo NMR Spectrum of Molybdate. Figure 1 shows the two signals present in the ^{95}Mo NMR spectrum of sodium molybdate at pH 6. When an alkaline solution of molybdate
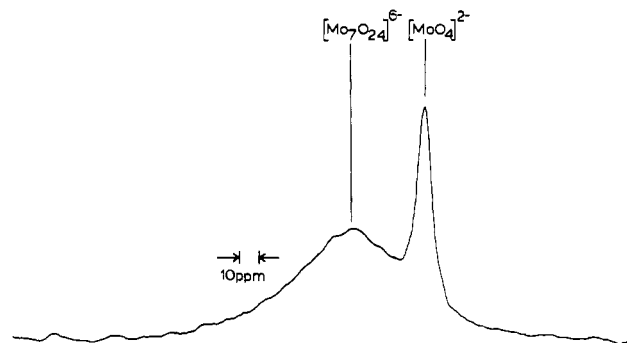

Figure 1. ^{95}Mo NMR spectrum of 1 M Na₂MoO₄·2H₂O in H₂O at pH 6. The width of the MoO₄$^{2-}$ line is slightly broadened by the weighting function applied for signal to noise enhancement.

is acidified, the sharp single line of MoO₄$^{2-}$ begins to broaden at pH 8, as found by Vold and Vold[25] in their ^{95,97}Mo NMR study. Below pH 6.5 the broad second line appears at +40 ± 6 ppm, and both resonances broaden further with decreasing pH. As pH is reduced below 5.3, both lines become unobservable with our equipment. The area ratios of the signals at five pH values between 5.3 and 6.4 are in very good agreement with the [MoO₄$^{2-}$]:[Mo₇O₂₄$^{6-}$] ratios calculated from the equilibrium constants in ref 4, supporting the assignment of Figure 1. An earlier study[26] of this pH region

(25) Vold, R. R.; Vold, R. L. *J. Magn. Reson.* **1975**, *19*, 365.
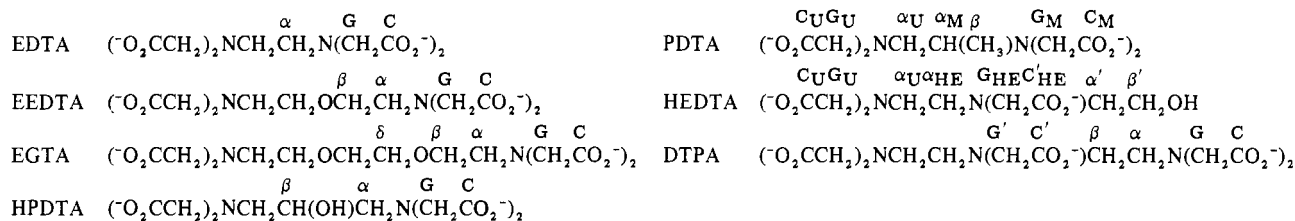(26) Kautt, W. D.; Kruger, H.; Lutz, O.; Maier, H.; Nolle, A. *Z. Naturforsch. A* **1976**, *31A*, 351.

Table III

¹³C NMR Chemical Shifts[a] of Protonated and Complexed Forms of Ligands (L) Which Can Form 1:1 and 2:1 Oxomolybdenum(VI) Complexes

L	Mo^VI:L	type[e]	C H+	C MoO₃	G H+	G MoO₃	α H+	α MoO₃	β H+	β MoO₃	other H+	other MoO₃
EDTA	0:1		171.80		59.27		52.79					
	1:1		171.57	178.33	58.80	63.38	51.85	56.92				
	2:1			178.77		63.56		57.69				
EEDTA	0:1		172.39		59.71		56.13		66.41			
	1:1		171.54	179.42	58.79	64.33[c]	56.21	62.89	65.89	68.45		
	2:1			179.33		64.33		62.69		68.26		
EGTA	0:1		171.49		58.13		55.88		65.87		(δ) 71.01	
	1:1		171.49[b]	179.30[c]	58.66	64.29[c]	55.98	62.29	65.87[b]	68.12	(δ) 70.94	70.75[c]
	2:1			179.30		64.29		62.25		68.02	(δ)	70.75
HPDTA	0:1		171.32		58.91		58.65		62.28			
	1:1		171.44	179.27[d] 178.74[d]	58.58	65.79 65.17	59.18	64.19		63.11		
	2:1			179.53[d] 178.97[d]		66.95 65.57				67.72		
PDTA	0:1	U	172.11		59.22		57.51					
		M	172.95		55.67		58.20		12.13			
	1:1/II	U	171.66		58.75		59.02					
		M		178.89[d] 178.78[d]		64.34[d] 63.34[d]		55.54		15.12		
	1:1/I	U		178.34[d] 178.23[d]		63.85[d] 63.34[d]		59.92				
		M	171.50		55.54		59.74		15.54			
	2:1	U		179.42[d] 179.31[d]		62.05[d] 61.87[d]		60.86				
		M		179.31[d] 179.12[d]		65.48[d] 65.22[d]		60.47		19.35		
HEDTA	0:1	U	172.10		59.03		52.43				(α') 58.62	
		HE	171.79		57.35		52.76				(β') 57.04	
	1:1	U		178.37		63.52		51.30			(α') 57.90	
		HE	171.85		57.47		56.83				(α') 57.90	
	2:1/I	U		179.05[d] 178.98[d]		63.78[d] 63.56[d]		54.42				
		HE		178.86		57.77					(α') (β')	61.05 70.04
	2:1/II	U		179.05[d] 178.91[d]		63.49[d] 63.35[d]		53.34				
		HE		178.84		57.77					(α') (β')	61.05 70.04
DTPA	0:1		171.82		58.23		54.11		50.36		(C') 179.51 (G') 57.46	
	1:1		173.03	179.00	57.73	63.77	53.39	59.90	49.91	51.03	(C') 178.41 (G') 57.74	
	2:1			178.60		63.65		58.06		51.18	(C') 174.21 (G') 58.06[c]	

Molecular Positions

EDTA
α G C
(⁻O₂CCH₂)₂NCH₂CH₂N(CH₂CO₂⁻)₂

EEDTA
β α G C
(⁻O₂CCH₂)₂NCH₂CH₂OCH₂CH₂N(CH₂CO₂⁻)₂

EGTA
δ β α G C
(⁻O₂CCH₂)₂NCH₂CH₂OCH₂CH₂OCH₂CH₂N(CH₂CO₂⁻)₂

HPDTA
β α G C
(⁻O₂CCH₂)₂NCH₂CH(OH)CH₂N(CH₂CO₂⁻)₂

PDTA
CU GU αU αM β GM CM
(⁻O₂CCH₂)₂NCH₂CH(CH₃)N(CH₂CO₂⁻)₂

HEDTA
CU GU αU αHE GHE CHE α' β'
(⁻O₂CCH₂)₂NCH₂CH₂N(CH₂CO₂⁻)CH₂CH₂OH

DTPA
G' C' β α G C
(⁻O₂CCH₂)₂NCH₂CH₂N(CH₂CO₂⁻)CH₂CH₂N(CH₂CO₂⁻)₂

[a] In ppm vs. external Me₄Si recorded in solutions of pH 6. [b] Unresolved from resonance of free ligand under experimental conditions. [c] Unresolved from resonance of 2:1 complex under experimental conditions. [d] Anisochronous carbon atoms. [e] Complex type and carbon atom identification.

did not detect both signals simulatneously.

⁹⁵Mo NMR of Complexes. Spectral findings are reported in Table IV.

¹⁷O NMR of Complexes. Spectral findings are reported in Table V.

Discussion

1:1 Mo(VI)–Ligand Complexes: IDA, MIDA, EtIDA, BzIDA, HEIDA, His, Asp. Ligands which contain a single iminodiacetate group form strong 1:1 complexes with Mo(VI). The expected manner of binding is facial tridentate coordi-

nation of the ligand to the trioxomolybdenum(VI) group as shown in I. This structure was proposed in earlier ¹H NMR
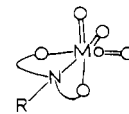
I

studies of the IDA,[27] MIDA,[17] and EDTA[28] complexes and

(27) Kula, R. J. *Anal. Chem.* **1967**, *39*, 1171.

Table IV. ^{95}Mo NMR Chemical Shifts and Line Widths and Solution Viscosities for Oxomolybdenum(VI) Complexes

complex	ppm^a	fwhm, Hz	η, cP	fwhm/η
(MoO₃)IDA²⁻	66 ± 2	128 ± 4^c	1.16	110 ± 5
(MoO₃)MIDA²⁻	63 ± 2	116 ± 6^c	0.99	117 ± 7
(MoO₃)EtIDA²⁻	67 ± 1	(160 ± 20)^b		
(MoO₃)BzIDA²⁻	65 ± 3	208 ± 20^c	1.10	189 ± 20
(MoO₃)NTA³⁻	67 ± 2	160 ± 15^c	1.08	148 ± 15
(MoO₃)Asp²⁻	NO^d			
(MoO₃)His⁻	NO^d			
(MoO₃)EDTA⁴⁻	63 ± 2	290 ± 20^c	2.45	118 ± 8
(MoO₃)₂PDTA⁴⁻	67 ± 2	260 ± 10^c	1.76	148 ± 6
(MoO₃)₂EEDTA⁴⁻	64 ± 2	154 ± 20^c	1.60	96 ± 13
(MoO₃)₂EGTA⁴⁻	64 ± 2	240 ± 30	1.92	125 ± 15
(MoO₃)₂HPDTA⁴⁻	70 ± 4	(400 ± 50)^b		
(MoO₃)₂HEDTA³⁻	76 ± 5	(500 ± 60)^b		

^{a} Chemical shift. Measured relative to external 1 M Na₂MoO₄ at pH 12. ^{b} As line width correlates strongly with viscosity and small differences in preparation of samples lead to large changes in viscosity, these results cannot be compared directly to the others. ^{c} Average of triplicate determinations on three separate occasions, ±σ. ^{d} ^{95}Mo resonance for molybdate is broadened by addition of ligand.

Table V. ^{17}O NMR Chemical Shifts, Line Widths, and Areas for Oxomolybdenum(VI) Complexes

complex	chem shift, ppm^a	fwhm, Hz	rel area
MoO₃NTA³⁻	701.5 ± 0.5	44	3.0
(MoO₃)₂EDTA⁴⁻	707.0 ± 0.5	110	2.0
	690.0 ± 0.5	66	1.0
MoO₃IDA²⁻	701.0 ± 2	175	
MoO₃MIDA²⁻	709.5 ± 0.5	48	2
	686.5 ± 0.5	32	1
MoO₃EDDA²⁻	704.0 ± 0.5	33	1
	689.0 ± 0.1	66	2

^{a} Measured relative to solvent H₂O.
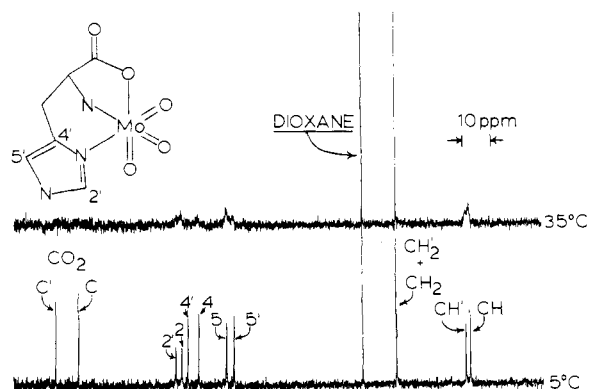
Figure 2. ^{13}C NMR spectra of 0.5 M histidine and 0.5 M Na₂MoO₄·2H₂O at 5 and 35 °C and pH 6. Dioxane line served as internal reference. Primed symbols (C′) identify lines from the complexed ligand. Unprimed lines are from free ligand.

confirmed in the solid state for the 2:1 complex Na₄(MoO₃)₂EDTA·8H₂O,[29] and the 1:1 complex, K₃(MoO₃)NTA·H₂O.[30] Histidine and aspartate form complexes of intermediate stability that contain one five-membered glycinate ring and one six-membered chelate ring terminating in either the N-3 atom of the imidazole ring in histidine (Figure 2) or the O atom of the β-carboxylate group in aspartate (II). A similar structure involving a seven-membered chelate ring probably exists for the recently described Mo(VI)–glutamate complex.[31] The larger ring in these complexes should be less
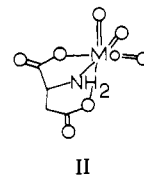

II

stable than the five-membered glycinate ring. This feature would account for previous reports of the histidine,[32,33] aspartate,[31,33] and glutamate[31] species as 1:1 Mo(VI)–ligand complexes of moderate stability, while potentiometric studies[34,35] have found that iminodiacetate complexes are very stable. Dipicolinic acid (DPA) (III), CYDTA, and the po-
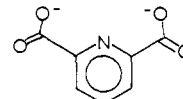
III

tential mono- and bidentate ligands in the first column of Table I do not coordinate to Mo(VI) in aqueous solution at pH 6. The failure of DPA to form a complex indicates that the oxo groups of MoO₃ do not rearrange to accommodate the meridional structure imposed by this ligand. For CYDTA, models show that facial MoO₃ cannot be fit to a given, equatorial IDA group because of the steric requirements of the other, gauche site. Apparently, coordination of the two nitrogens and coordination of the carboxylate ligands does not occur, perhaps because of unfavorable desolvation of the other carboxylates.

The foregoing results suggest that all elements of structure I, i.e., firm coordination in a facial arrangement by three donor atoms from a single chelating ligand, are needed to stabilize (MoO₃)L^{n-} complexes in solution. The ligands in the second column of Table I meet these requirements. If, however, one (or more) of the coordination sites available on MoO₃ is not firmly occupied by a ligand donor atom, coordination of water or hydroxide ion causes reversion to tetrahedral MoO₄²⁻ or (at lower pH) molybdate polymerization. Zare et al.[36] proposed such reversion in alkaline media from kinetic studies of the dissociation of (MoO₃)EDTA⁴⁻. We conclude that a reaction such as (1) is responsible for the reduced stability of

(1)
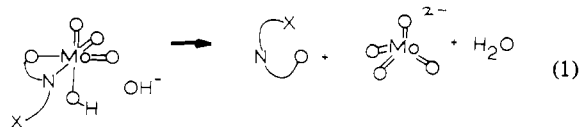
MoO₃ complexes with histidine, aspartate, and glutamate and the failure to observe MoO₃ complexes with CYDTA, DPA, and the mono- and bidentate ligands in Table I.

One of the above complexes deserves special comment. Spectra of the 1:1 Mo(VI)–histidine complex reported at 5 and 35 °C in Figure 2 demonstrate that this species is intermolecularly labile. A condition of such intermediate exchange has been observed previously only for the (MoO₃)(cysteine)²⁻ complex[37] and is unlike the behavior of the iminodiacetate complexes, which are inert to intermolecular exchange on the time scale of these experiments.

N,N′-EDDA. Coordination of N,N′-EDDA produces two structural isomers (IN and OUT, see Figure 3) which differ

(28) Kula, R. J. *Anal. Chem.* **1966**, *38*, 1581.
(29) Park, J. J.; Glick, M. D.; Hoard, J. L. *J. Am. Chem. Soc.* **1969**, *91*, 301.
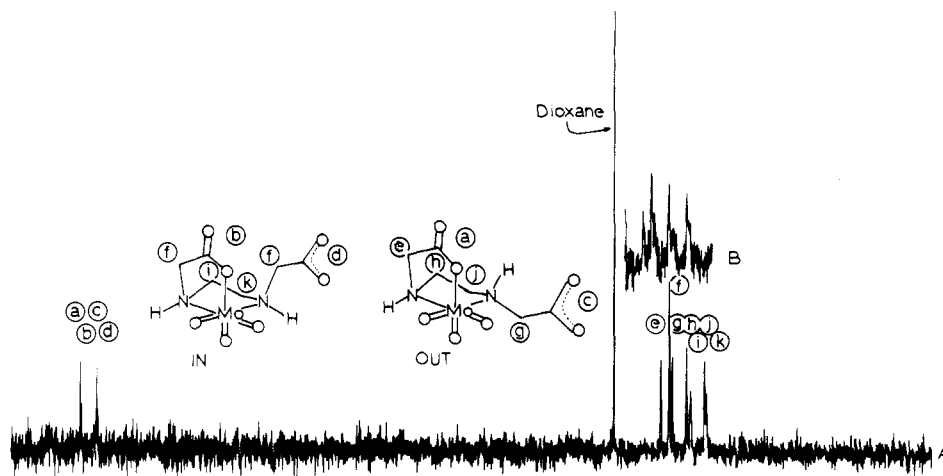(30) Butcher, R. J.; Penfold, B. R. *J. Cryst. Mol. Struct.* **1976**, *6*, 13.
(31) Rabinstein, D. L.; Greenberg, M. S.; Saetre, R. *Inorg. Chem.* **1977**, *16*, 1241.
(32) Spence, J. T.; Lee, J. Y. *Inorg. Chem.* **1965**, *4*, 385.
(33) Butcher, R. J.; Powell, H. K. J.; Wilkins, C. J.; Yong, S. H. *J. Chem. Soc., Dalton Trans* **1976**, 356.
(34) Kula, R. J.; Rabinstein, D. L. *Anal. Chem.* **1966**, *38*, 1934.
(35) Zare, K.; Lagrange, P.; Lagrange, J. *J. Chem. Soc., Dalton Trans.* **1979**, 1372.
(36) Zare, K.; Lagrange, J.; Lagrange, P. *Inorg. Chem.* **1979**, *18*, 568.
(37) Callis, G. E.; Wentworth, R. A. D. *Bioinorg. Chem.* **1977**, *7*, 57.

Figure 3. ^{13}C NMR spectra of 0.5 M N,N'-EDDA and 0.5 M $Na_2MoO_4\cdot2H_2O$ at (A) ambient temperature ($\sim$35 °C) and (B) elevated temperature ($\sim$55 °C). Note that lines i and k are the broadest lines in the ambient temperature spectrum and become broader with elevated temperature, indicative of exchange broadening.
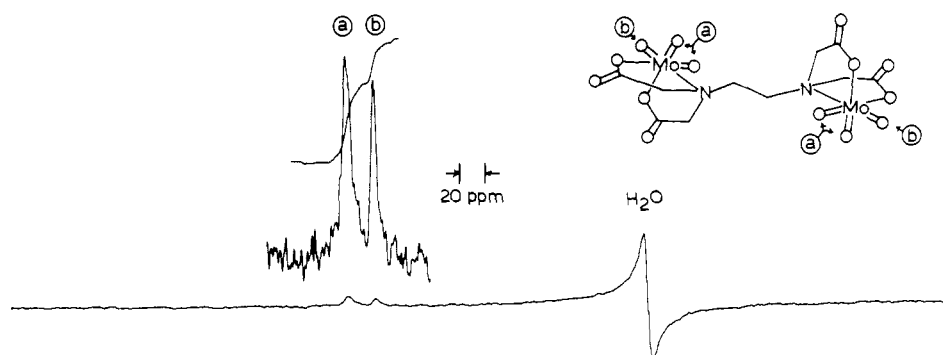

Figure 4. ^{17}O NMR spectrum of 0.6 M $Na_4[(MoO_3)_2EDTA]$ at pH 6.0. Sample prepared from recrystallized solid complex. Reference water line is folded back into the spectrum by 491 ppm because of limited 10-KHz sweep width. The water line is out of phase with the rest of the spectrum due to the sharp rolloff of receiver gain outside the sweep range caused by a noise-reducing crystal filter. See ref 20 for details. This feature served to increase the relative size of the $(MoO_3)_2EDTA$ signals.

Scheme I

Scheme II
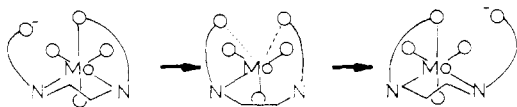
in the orientation of the pendant chelate arm relative to the "V" made by the three coordinated arms. The resolution of the spectra for the two isomers demonstrates a relatively nonlabile Mo–N bond as lability in the Mo–N bond should lead to inversion of the nitrogen closest to the free arm and subsequent interconversion of the two isomers. The assignment of the more intense lines to the OUT form (Roman numeral I in Table II) was made on the basis of the large width of the ethylene lines for the less abundant species and the apparent equivalence of the glycinate carbons. The IN species is oriented for a particularly fast exchange of bound and free carboxylate arms as shown in Scheme I, suggesting that it be the more rapidly exchanging species.

IDA and NTA. Detailed carbon-13 and proton NMR studies[24] found the solution structure of MoO_3NTA^{3-} to be like I with a free, pendant glycinate arm. This conformation also occurs in the crystal structure of the complex.[30] Rapid exchange of the free and bound glycinate arms produces the single, averaged carbon-13 signals reported in Table II.

A single oxygen-17 NMR signal has been observed[38] for the three oxo ligands on molybdenum in MoO_3NTA^{3-}. The relatively inert MoO_3IDA^{2-} complex also provides a single-line
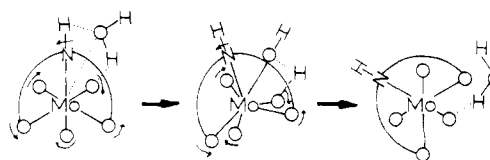
oxygen spectrum, but with greater line width than the NTA signal. Table V reports single lines for both of these complexes at pH 6. However, the spectrum of $(MoO_3)_2EDTA^{4-}$, displayed in Figure 4, consists of two signals with a 2:1 area ratio. The signals arise from the two oxo groups trans to carboxylate and the one trans to amine. The chemical shift of the MoO_3NTA^{3-} complex is precisely the weighted average of the shifts of the two signals of the EDTA complex. The oxos of the NTA complex therefore undergo fast exchange between positions trans to amine and trans to carboxylate but not with solvent water.

The oxygen-17 signal from MoO_3IDA^{2-} is a broad asymmetric line at the same chemical shift as the MoO_3NTA^{3-} signal. Although the IDA complex has been shown to undergo intermolecular exchange at pH >8, the complex is inert to such exchange at pH 6.[27] The IDA ligand is judged to be coordinated almost all of the time under the latter condition because ABX coupling is observed for the NH and CH_2 protons in the glycinate arms of the complex.[27] However, the single peak in the ^{17}O spectrum demonstrates that positional exchange takes place among the three oxos of MoO_3IDA^{2-} at pH 6. The above facts indicate that neither partial dissociation of the chelate nor fast exchange of oxo ligands with solvent

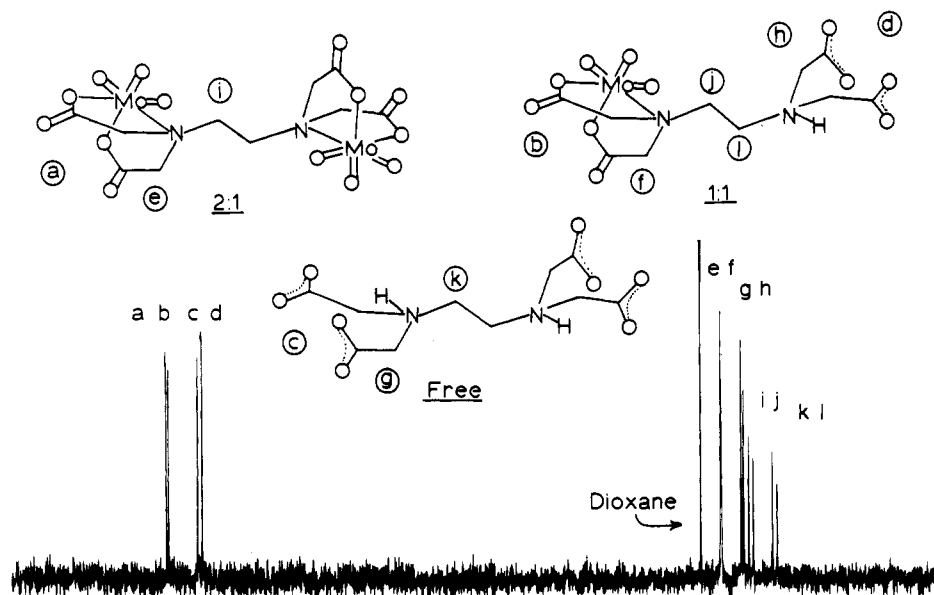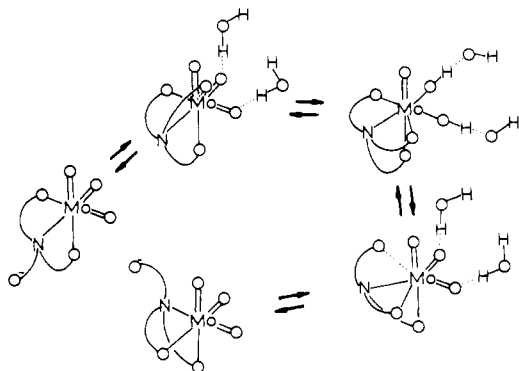(38) Miller, K. F.; Wentworth, R. A. D. *Inorg. Chem.* **1979**, *18*, 984.

Figure 5. ^{13}C NMR spectrum of 0.5 M EDTA and 0.5 M Na₂MoO₄·2H₂O at pH 6 in 20% H₂O/D₂O solution.

Scheme III

can be responsible for this behavior. Scheme II suggests a trigonal twist mechanism involving solvent water and the IDA amine proton to explain the observed equivalence.

The mechanism shown in Scheme III is proposed to explain the related oxo scrambling found in MoO₃NTA³⁻. Solvent has been demonstrated to play an important role in this rearrangement,[38] but unlike the previously proposed mechanisms, we suggest that scrambling originates with nucleophilic attack of the free glycinate arm. This weakens the oxo–molybdenum bonds along the equatorial edge of the octahedral face adjacent to the attack. The weakened Mo=O bonds make these oxos more susceptible to protonation by the solvent, becoming essentially singly bonded hydroxyl groups. The seven-coordinate intermediate adopts pentagonal-bipyramidal geometry because of the ring constraints of NTA. However, formation of two coplanar glycinate rings in the intermediate produces sufficient strain to break one of the carboxylate–molybdenum bonds. Relaxation of the complex to octahedral coordination results in return of the protons to the solvent. The proposed seven-coordinate pentagonal-bipyramidal intermediate is structurally similar to known Mo(VI) complexes[6,39] and provides for retention of one five-membered chelate ring throughout the interchange of oxo positions.

Ligands Forming 2:1 and 1:1 Complexes with Mo(VI): EDTA, EEDTA, and EGTA. The symmetric chelators EDTA, EEDTA, and EGTA represent the simplest class of ligands which may form 2:1 complexes with Mo(VI). At metal:ligand

ratios of 2:1 and greater, these ligands quantitatively form complexes in which each IDA group coordinates MoO₃ in a facial tridentate manner. At lower metal:ligand ratios, 1:1 complexes such as (MoO₃)EDTA(H⁺)³⁻ also exist, as was determined from proton NMR studies.[28] The chemical and ^{13}C NMR spectral properties of individual IDA groups are influenced by the status of the second IDA site in the molecule. At pH 6 in these experiments the two N atoms of free EDTA are almost completely protonated.[28] Coordination of one MoO₃ group results in the molecule (⁻O₂CCH₂)₂NH⁺-CH₂CH₂N(CH₂CO₂⁻)₂(MoO₃). Displacement of one proton by MoO₃ produces substantial downfield shifts in the resonances of carbon atoms in the vicinity of the coordination site; small, pH-dependent, and generally upfield shifts occur in the signals from the unmetalated end of the molecule, indicating further protonation at this site (see Table III). Addition of a second MoO₃ group removes the proton from the second IDA site and causes large downfield shifts in the signals of atoms in the vicinity of this change and smaller shifts in signals from other atoms throughout the molecule.

The chemical properties of an IDA site depend on whether H⁺ or MoO₃ is coordinated at the opposite end of the molecule. Kula's results[28] show that replacement of H⁺ by MoO₃ on one end of EDTA(H⁺)₂²⁻ increases the basicity of the bare iminodiacetate group by a factor of 20 but reduces its tendency to coordinate MoO₃ by a factor of about 3. However, formation of the 2:1 Mo(VI)–EDTA complex is still possible in solutions containing a 1:1 mole ratio of metal to ligand owing to the equilibrium

$$2(MoO_3)EDTA(H^+) \rightleftharpoons$$
$$(MoO_3)_2EDTA^{4-} + EDTA(H^+)_2^{2-} \quad (2)$$
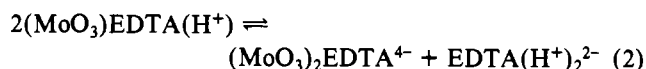
The equilibrium constant for reaction 2 is $\sim^1/_{13}$.[28] The changes in chemical shift that result when H⁺ is displaced by MoO₃ at an iminodiacetate site on EDTA produce a clear separation of the C atom resonances possible for the species shown in reaction 2. Thus, in a 1:1 Mo(VI)–EDTA solution at pH 6, 12 separate ^{13}C resonances are observed owing to the presence of free ligand (3 lines), 1:1 complex (6 lines), and 2:1 complex (3 lines) as shown in Figure 5.

Interaction between IDA groups in EEDTA and EGTA diminishes because of the greater distance between coordination sites. However, 15 of 16 and 15 of 20 possible resonances are observed in 1:1 Mo(VI)–EEDTA and Mo(VI)–EGTA solutions, respectively, at pH 6 (Table III). No evi-

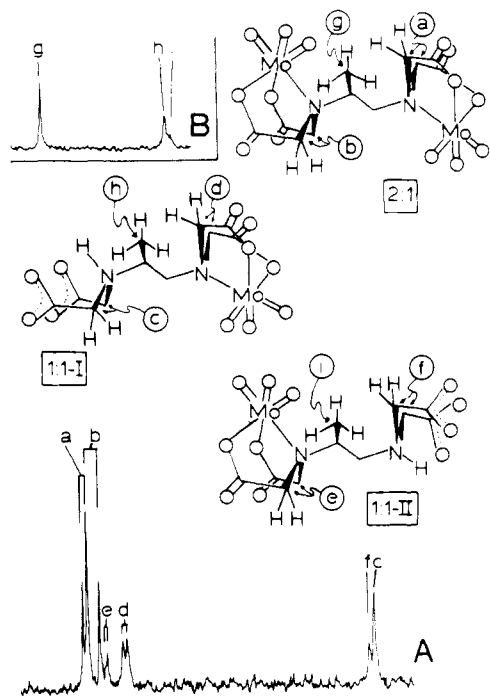(39) Wieghardt, K.; Holzbach, W.; Hofer, E.; Weiss, J. *Inorg. Chem.* **1981**, *20*, 343.

Figure 6. (A) Carboxyl region of ^{13}C NMR spectrum of 0.5 M PDTA and 0.75 M $Na_2MoO_4\cdot2H_2O$ at pH 6 in 20% D_2O/H_2O solution and (B) methyl region of the same sample. Drawings indicate spatial arrangement of the PDTA ligand suggested by the size of the separation between carboxyl lines of a given species. The protonated forms of the ligand undergo rapid inversion of the uncomplexed nitrogen and the two different glycinate arms shown become equilibrated.

dence is seen for ethereal oxygen coordination by these ligands, in keeping with the inability of diglycolic acid to form a complex.

HPDTA. The complexation behavior of HPDTA is similar to that of the above three ligands. However, the hydroxyl group on the trimethylene backbone causes the carboxylate and glycinate carbons within a coordinated IDA group to be inequivalent. Coordination to MoO_3 fixes the acetate arms in a single conformation, and the carboxylate and glycinate carbons become magnetically inequivalent (anisochronous), yielding pairs of ^{13}C lines (see Table III). Protonated sites do not exhibit this differentiation because rapid inversion of the nitrogen atom interchanges the two types of glycinate arms.

PDTA. In PDTA the methyl substituent on the ethylene linkage causes the two IDA groups to become chemically distinct and the glycinate and carboxylate carbons of each IDA group to become magnetically inequivalent upon coordination. ^{13}C NMR reveals that the two IDA sites differ in their tendency to coordinate molybdate. The carboxyl region from the spectrum of a solution containing Mo(VI) and PDTA in a 1.5:1 ratio exhibits three sets of lines (Figure 6A, Table III). Uncoordinated ligand is not present in this solution. One set of four lines is attributed to anisochronous carbons a and b found at the two IDA sites of the 2:1 complex. A second set of three lines is assigned to the type I 1:1 complex in which MoO_3 coordinates to the IDA group further from the methyl substituent (pair d) and the other end is protonated (single line c). The three lines of the type II 1:1 complex result from coordination at the end nearer to the methyl group (pair e) and protonation of the opposite end of the molecule I (single line f). As type I signals are more intense than type II, MoO_3 coordination further from the methyl group is apparently favored. Proton NMR results[28] and the X-ray crystal structure[29] of $(MoO_3)_2EDTA^{4-}$ show that a trans orientation of the NCH_2CH_2N linkage is favored in the coordinated state. As depicted in Figure 6, in this conformation the coordinated

acetate arms in the structure 1:1-I, where the MoO_3 moiety occupies the $CH(CH_3)CH_2IDA$ site, are closer to the methyl group than the coordinated glycinate arms of the $CH_2CH-(CH_3)IDA$ site in structure 1:1-II. The more abundant species is the one exhibiting the greater splitting of coordinated carboxylate resonances and is assigned to the complex formed by the less sterically hindered end of the molecule.

DTPA. DTPA forms molybdate complexes only with the IDA moieties of the molecule; the central glycinate arm does not participate in coordination. At pH 6 the free ligand exists as a diprotonated species with the terminal nitrogen atoms bearing most of the charge.[40] Upon coordination of MoO_3 to one IDA group, protons distribute more evenly between the remaining N atoms but still favor the end nitrogen. Complexation of the second IDA site leads to almost complete protonation of the central nitrogen atom. These effects are clearly manifested in the chemical shifts reported in Table III. The downfield shifts at terminal sites and upfield shifts at the central site enforced by MoO_3 coordination confirms the complicated protonation behavior of DTPA reported from ^{13}C NMR titration by Sarneski and Reilley.[41]

Ligands Which Form $Mo_2O_5^{2+}$ Complexes: MHEG and HEDTA. MHEG forms two structurally distinct weak complexes with Mo(VI) which are inert on the NMR time scale. The 13.5-ppm downfield shift of the hydroxyl carbon resonance in both species (Table II) indicates coordination of the hydroxyethyl arm, which fulfills the tridentate requirement for stable coordination to oxomolybdenum(VI), although hydroxyl coordination is less favored than carboxylate coordination as shown by the absence of hydroxylethyl coordination in the Mo(VI)–HEIDA complex (Table II). The formation of two complexes by MHEG contrasts with the behavior of other tridentate ligands which form only a single complex with molybdate.

HEDTA has one IDA and one N-(hydroxyethyl)glycine coordination site. The 1:1 complex forms exclusively at the IDA end (Table III) in agreement with the relative stabilities of the MIDA and MHEG complexes. The carboxyl region of the ^{13}C NMR spectrum of this complex is shown in Figure 7A. In solutions containing Mo(VI) and HEDTA in a ratio of 2.5:1 or greater, two 2:1 Mo(VI)–HEDTA complexes form, just as two MHEG complexes form in 1:1 solutions of MHEG. The 13-ppm downfield shift of the hydroxyl-bearing methylene carbon signal indicates coordination of the CH_2CH_2OH arm in the HEDTA species as well. The carboxylate region of the ^{13}C NMR spectrum of a 2.5:1 Mo(VI)–HEDTA solution contains two three-line sets of resonances as shown in Figure 7B. Each set contains a pair of lines for the carboxylate carbons of the coordinated IDA group, made anisochronous by the asymmetry of the second coordinated nitrogen, and a single line for the carboxylate carbon in the coordinated (hydroxyethyl)glycine moiety.

The existence of two types of 1:1 Mo(VI)–MHEG and 2:1 Mo(VI)–HEDTA complexes is attributed to formation of an oxo-bridged $Mo_2O_5^{2+}$ unit by the coordinated hydroxyethylglycine site in each molecule. Formation of a dimeric $Mo_2O_5^{2+}$ species from MoO_3MIDA^{2-} and MoO_3NTA^{3-} has been noted previously at pH ≤ 2.[17,42,43] Deprotonation of the CH_2CH_2OH arm upon coordination enables the formation of such species with MHEG and HEDTA at pH 6. Potentiometric pH ti-

(40) Sudmeier, J. L.; Reilley, C. N. *Anal. Chem.* **1964**, *36*, 1698.
(41) Sarneski, J. E.; Reilley, C. N. In "Analytical Chemistry: Essays in Memory of Anders Ringbom"; Wanninen, E., Ed.; Pergamon Press: New York, 1977; p 35.
(42) Knobler, C.; Matheson, A. J.; Wilkins, C. J. "Molybdenum Chemistry of Biological Significance"; Newton, W. E., Otsuka, S., Eds.; Plenum Press: New York, 1980; pp 319–325.
(43) Knobler, C.; Penfold, B. R.; Robinson, W. T.; Wilkins, C. J.; Yong, S. H. *J. Chem. Soc., Dalton Trans.* **1980**, 248.
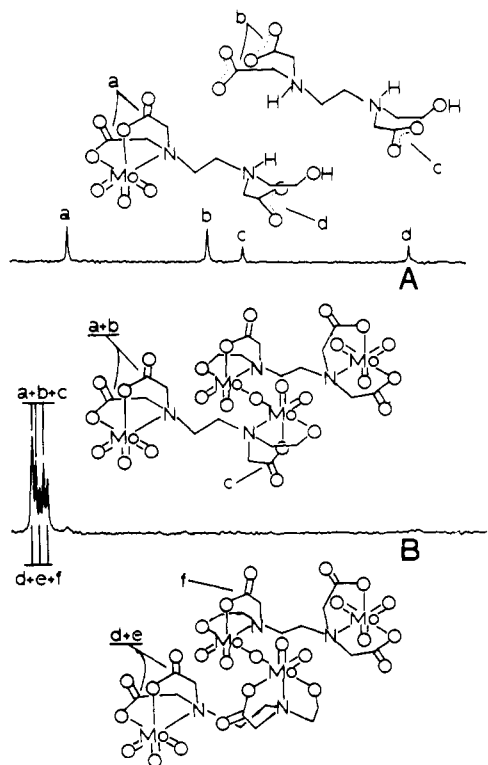
Figure 7. (A) Carboxyl region of ^{13}C NMR spectrum of 0.5 M HEDTA and 0.25 M $Na_2MoO_4 \cdot 2H_2O$ at pH 6 in 20% D_2O/H_2O solution and (B) carboxyl region of ^{13}C NMR spectrum of 0.5 M HEDTA and 1.25 M $Na_2MoO_4 \cdot 2H_2O$ at pH 6 in 20% D_2O/H_2O solution.

trations of molybdate and ligand confirm the loss of this proton from the following stoichiometry:

$$4MoO_4^{2-} + 2HEDTA^{3-} + 8H^+ \rightarrow$$
$$(O_3Mo)HEDTA(Mo_2O_5)HEDTA(MoO_3)^{6-} + 5H_2O \quad (3)$$
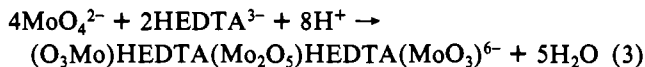
Thus, the complexes actually exist as the 2:2 and 4:2 species $MHEG(Mo_2O_5)MHEG^{2-}$ and $(O_3Mo)HEDTA(Mo_2O_5)$-$HEDTA(MoO_3)^{6-}$. Dimerization of the coordinated (hydroxyethyl)glycine sites produces diasterisomers which are discernible by NMR.
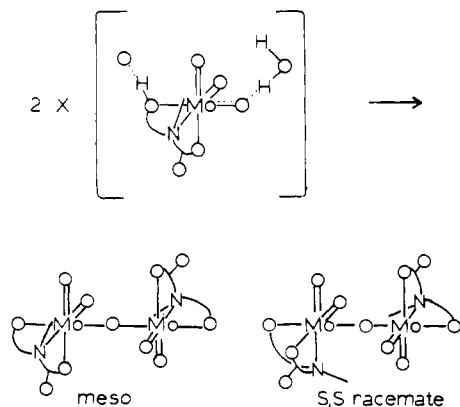
Steric considerations suggest that the meso form is favored; thus the larger type I lines of the MHEG complex and 4:2 Mo(VI)–HEDTA complex are assigned to this form and the smaller type II lines to the racemic forms. Assignment of lines in the carboxylate region of the 4:2 Mo(VI)–HEDTA complex is shown in Figure 7B.

Trans Influence and Oxygen-17 NMR Spectroscopy. The trans influence of a coordinating group is a measure of the extent to which that group weakens the metal–ligand bond trans to itself. We have examined X-ray structural data from

21 Mo(VI) complexes[5,8,10,29,30,44-57] and have determined a ranking of trans-influencing ability for common ligand groups based on the length of the bond trans to that group in compounds of similar structure and composition. The ranking is $N^{3-} > RN^{2-} \approx O^{2-} > \mu\text{-}O^{2-}$ (linear) $> RO^- \approx F^- > Cl^- > RS^- \gtrsim Br^- > R_3N \gtrsim RCO_2^- \gtrsim acac^- \gtrsim R_2S > H_2O > ROH$. This sequence follows the expected electron-donating abilities of the ligands. The MHEG and HEDTA ligands discussed above form dimeric $Mo_2O_5^{2+}$ complexes because the trans-influencing ability of coordinated alkoxy is sufficient to weaken the opposing $Mo\!\!=\!\!O$ bond in the oxometal core to the point where μ-oxo bridge formation is possible. A further consequence of the trans influence is that one finds the $CH_2CH_2O^-$ and μ-oxo groups trans to one another and weakly donating amine and carboxylate groups trans to $Mo\!\!=\!\!O$ in the $Mo_2O_5^{2+}$ complexes. The trans influence therefore is important in determining the oxo content of the core and the arrangement of other ligands in oxomolybdenum(VI) complexes. Examples of its effect can be seen in the variety of oxo centers—MoO_3, $Mo_2O_5^{2+}$, MoO_2^{2+}, $Mo_2O_3^{6+}$—which have been observed as stable Mo(VI) complexes,[2,5,33,39,42,43,49] and the types of arrangement of ligands therein. Kidd[58] found that ^{17}O chemical shifts of oxochromium(VI) species were linearly related to the chromium oxygen bond order, with stronger π bonds corresponding to larger downfield shifts. In Figure 4, the ^{17}O NMR spectrum of $(MoO_3)_2$ $EDTA^{4-}$ shows that the signals from the structurally inequivalent oxos of the MoO_3 moiety are resolved from one another. The solution basicities of the amine and carboxylate groups as indicated by the protonation behavior of the ligand[40] predict that the oxo ligand trans to amine will experience a greater trans influence than the oxo ligands trans to carboxylate. The smaller signal in Figure 4 occurs upfield of the larger and thus is less strongly π bonded. The assignment of the higher field line to the oxo trans to nitrogen is confirmed by reversal of the relative areas of the upfield and downfield lines in the ^{17}O spectrum of MoO_3EDDA^{2-}, where two oxo ligands are trans to amine and one is trans to carboxylate, as reported in Table V.

In Figure 8, ^{17}O chemical shifts of oxo ligand resonances are plotted as a function of molybdenum oxygen bond distances for a number of Mo(VI) oxo anions and complexes.[38,59] In

(44) Haymore, B. L.; Maatta, E. A.; Wentworth, R. A. D. *J. Am. Chem. Soc.* **1979**, *101*, 2063.
(45) Dirand, J.; Ricard, L.; Weiss, R. *Transition Met. Chem.* (*Weinheim, Ger.*) **1975**, *1*, 2.
(46) Ricard, L.; Estienne, J.; Karagiannidis, P.; Toledano, P.; Fischer, J.; Mitschler, A.; Weiss, R. *J. Coord. Chem.* **1974**, *3*, 277.
(47) Chatt, J.; Choukroun, R.; Dilworth, J. R.; Hyde, J.; Vella, P.; Zubieta, J. *Transition Met. Chem.* (*Weinheim, Ger.*) **1979**, *4*, 59.
(48) Bishop, M. W.; Chatt, J.; Dilworth, J. R.; Hursthouse, M. B.; Motevalli, M. *J. Chem. Soc., Dalton Trans.* **1979**, 1600.
(49) Cotton, F. A.; Morehouse, S. M.; Wood, J. S. *Inorg. Chem.* **1964**, *3*, 1603.
(50) Atovmyan, L. O.; Sokolova, Yu. A.; Tkachev, V. V. *Dokl. Akad. Nauk SSSR* **1970**, *195*, 1355; *Dokl. Phys. Chem.* (*Engl. Transl.*) **1970**, *195*, 968.
(51) Villa, A. C.; Loghi, L.; Mafredotti, A. G.; Guastini, C. *Cryst. Struct. Commun.* **1974**, *3*, 551.
(52) Grandjean, D.; Weiss, R. *Bull. Soc. Chim. Fr.* **1967**, *34*, 3049.
(53) Dirand, J.; Ricard, L.; Weiss, R. *J. Chem. Soc., Dalton Trans.* **1976**, 278.
(54) Dirand-Colin, J.; Schappacher, M.; Ricard, L.; Weiss, R. *J. Less-Common Met.* **1977**, *54*, 91.
(55) Yamanouchi, K.; Enemark, J. H. *Inorg. Chem.* **1979**, *18*, 1626.
(56) Kojic-Prodic,, B.; Ruzic-Toros, Z.; Grdenic, D.; Golic, L. *Acta Crystallogr., Sect. B* **1974**, *B30*, 300.
(57) Craven, B. M.; Ramey, K. C.; Wise, W. B. *Inorg. Chem.* **1971**, *10*, 2626.
(58) Kidd, R. G. *Can. J. Chem.* **1967**, *45*, 605.
(59) Filowitz, M.; Ho, R. K. C.; Klemperer, W. G.; Shum, W. *Inorg. Chem.* **1979**, *18*, 93.
(60) Cotton, F. A.; Wing, R. M. *Inorg. Chem.* **1965**, *4*, 867.
(61) Stadnicka, K.; Haber, J.; Kozlowski, R. *Acta Crystallogr., Sect. B* **1977**, *B33*, 3859.
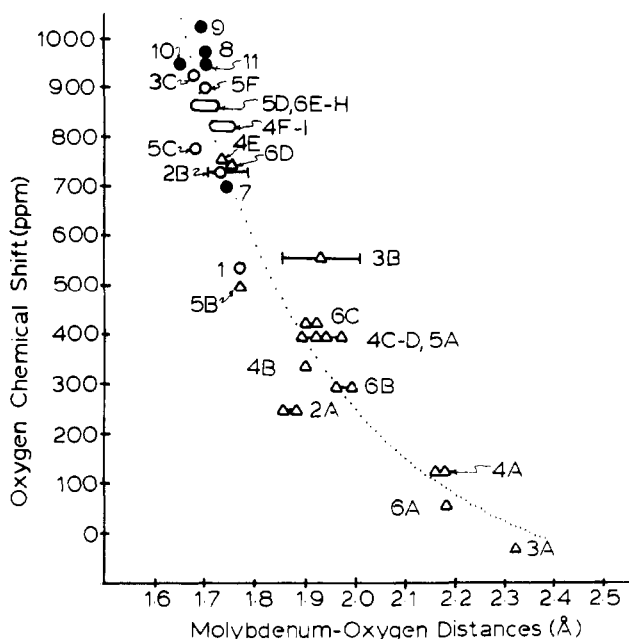(62) Allcock, H. R.; Bissell, E. C.; Shawl, E. T. *Inorg. Chem.* **1973**, *12*, 2963.

Figure 8. Oxygen-17 NMR chemical shifts of oxomolybdenum(VI) compounds plotted vs. the shortest oxygen–molybdenum separation found at each oxo ligand: O, terminal oxo ligands in oxo anions; ●, terminal oxo ligands found in oxomolybdenum complexes with other ligands present; △, bridging oxo ligands found in oxoanions. Structural data: (1) [MoO$_4{}^{2-}$], ref 60; (2) [Mo$_2$O$_7{}^{2-}$], ref 61; (3) [Mo$_6$O$_{19}{}^{2-}$], ref 62; (4) [Mo$_7$O$_{24}{}^{6-}$], ref 63; (5) [α-Mo$_8$O$_{26}{}^{4-}$], ref 64; (6) [β-Mo$_8$O$_{26}{}^{4-}$], ref 46; (7) [MoO$_3$(IDA)$^{2-}$], adapted from ref 29; (8) [MoO$_2$(S$_2$CNEt$_2$)$_2$], ref 65; (9) [MoO$_2$(acac)$_2$], ref 57; (10) [MoOCl$_2$(S$_2$CNEt$_2$)$_2$], ref 53; (11) [MoOBr$_2$(S$_2$CNEt$_2$)], ref 53. ^{17}O NMR data for oxoanions are from ref 59, where the letter beside each datum is that assigned to a given position. ^{17}O NMR data for oxomolybdenum complexes are from ref 38 and this work. The dotted line serves as guide to the nonlinearity of the relation between bond distances and chemical shifts.

instances where more than one Mo–O distance is observed in oxoanions for a given oxygen atom, the shortest Mo–O distance is plotted. Figure 8 shows a smooth, nonlinear relationship between chemical shift and bond distance. The sensitivity of the ^{17}O chemical shift to bonding environment is greatest at the downfield (more tightly bonded) end of the curve. Thus, differences in the electronic environment of multiply bonded oxo groups can be detected by oxygen-17 NMR when crystal structures reveal no difference in Mo—O bond lengths, as exemplified by resolution of ^{17}O=Mo signals in response to their trans-bonded ligand atoms in (MoO$_3$)$_2$EDTA^{4-}.

Bond distances greater than about 2.3 Å have little correlation with the oxygen-17 chemical shift value (such bond distances are ignored in Figure 8 where shorter ones exist). The value 2.32 Å is the average Mo–O distance found for oxo 3A in Mo$_6$O$_{19}{}^{3-}$ and is the most upfield resonance in Figure

8. It has been suggested that the π bond order of this oxo is 0.38 The octahedral symmetry of the site of this oxo ligand in Mo$_6$O$_{19}{}^{2-}$ (shown below) reduces the possible σ bond order to $^2/_3$. The very short, collinear terminal oxomolybdenum bonds no doubt promote an even weaker bond by their large trans influence. The 2.32-Å value therefore reflects a primarily electrostatic oxygen–molybdenum bond. It is fascinating to note that 2.32 Å is precisely the sum of the O^{2-} crystal radius and the Mo^{6+} univalent radius given by Pauling.66
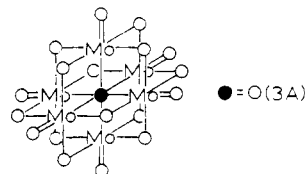
^{95}Mo Chemical Shifts and Line Widths. The ^{95}Mo chemical shifts reported for oxomolybdenum chelates in Table IV and for Mo$_7$O$_{24}{}^{6-}$ fall downfield of molybdate, just as ^{51}V signals of V$_{10}$O$_{28}{}^{6-}$ and VO$_2$(EDTA)$^{3-}$ fall downfield of VO$_4{}^{3-}$.67 The IDA-like complexes exhibit a range of chemical shifts of ±4 ppm around +66 ppm while the ethoxy-bond HEDTA complex is slightly farther downfield. The downfield shift with chelation is probably due to decreased electron density on Mo, as reflected in the stronger oxo bonding and higher ^{17}O shifts found in MoO$_3$(IDA)$^{2-}$ than MoO$_4{}^{2-}$.

The quotient of observed line width of ^{95}Mo signals and the intrinsic viscosity of the sample is constant for most complexes. NTA, BzIDA, and PDTA complexes display slightly higher values, perhaps due to the bulkiness of the substituents on the carbon α to the coordinated nitrogen or specifically to the lability of the NTA complex. The lack of correlation of corrected line widths to the molecular sizes of the complexes is surprising. Apparently the line widths are not controlled by rotations involving the entire R group of the R(IDA) complex.

(63) Evans, H. T.; Gatehouse, B. M.; Leverett, P. *J. Chem. Soc., Dalton Trans.* **1975**, 505.
(64) Fuchs, J.; Hartl, H. *Angew. Chem., Int. Ed. Engl.* **1976**, *15*, 375. Vivier, H.; Bernard, J.; Djomma, H. *Rev. Chim. Miner.* **1977**, *14*, 584.
(65) Berg, J. M.; Hodgson, K. O. *Inorg. Chem.* **1980**, *19*, 2180.

(66) Pauling, L. "The Nature of the Chemical Bond", 3rd ed.; Cornell University Press: Ithaca, NY, 1960.
(67) O'Donnell, S. E.; Pope, M. T. *J. Chem. Soc., Dalton Trans.* **1976**, 2290.